Mineralogical Magazine (2023), **87**, 695–701
doi:10.1180/mgm.2023.42

CAMBRIDGE UNIVERSITY PRESS

Article

Bakakinite, $Ca_2V_2O_7$, a new mineral from fumarolic exhalations of the Tolbachik volcano, Kamchatka, Russia

Igor V. Pekov[1], Atali A. Agakhanov[2], Natalia N. Koshlyakova[1], Natalia V. Zubkova[1], Vasiliy O. Yapaskurt[1], Sergey N. Britvin[3], Marina F. Vigasina[1], Anna G. Turchkova[1] and Maria A. Nazarova[4]

[1]Faculty of Geology, Moscow State University, Vorobievy Gory, 119991 Moscow, Russia; [2]Fersman Mineralogical Museum of the Russian Academy of Sciences, Leninsky Prospekt 18-2, 119071 Moscow, Russia; [3]Dept. of Crystallography, St Petersburg State University, University Embankment 7/9, 199034 St Petersburg, Russia; and [4]Institute of Volcanology and Seismology, Far Eastern Branch of Russian Academy of Sciences, Piip Boulevard 9, 683006 Petropavlovsk-Kamchatsky, Russia

Abstract

The new mineral bakakinite, ideally $Ca_2V_2O_7$, was found in the high-temperature (not lower than 500°C) exhalations of the Arsenatnaya fumarole at the Second scoria cone of the Northern Breakthrough of the Great Tolbachik Fissure Eruption, Tolbachik volcano, Kamchatka, Russia. It is associated with anhydrite, svabite, pliniusite, schäferite, berzeliite, diopside, hematite, powellite, baryte, fluorapatite, calciojohillerite, ludwigite, magnesioferrite, anorthite, titanite and esseneite. Bakakinite forms flattened crystals up to 30 × 5 μm, typically distorted. The mineral is transparent, colourless or pale yellow, with strong vitreous lustre. Electron microprobe analysis gave (wt.%): CaO 37.04, SrO 0.26, SiO_2 0.16, P_2O_5 1.48, V_2O_5 49.47, As_2O_5 10.85, SO_3 0.35, total 99.61. The empirical formula calculated on the basis of 7 O apfu is $(Ca_{1.99}Sr_{0.01})_{\Sigma 2.00}(V_{1.64}As_{0.28}P_{0.06}Si_{0.01}S_{0.01})_{\Sigma 2.00}O_7$. The D_{calc} is 3.463 g cm^{-3}. Bakakinite is triclinic, $P\bar{1}$, unit-cell parameters are: $a = 6.64(2)$, $b = 6.92(2)$, $c = 7.01(2)$ Å, $\alpha = 86.59(7)$, $\beta = 63.77(7)$, $\gamma = 83.47(6)°$, $V = 287.0(5)$ Å^3 and $Z = 2$. The strongest reflections of the powder X-ray diffraction pattern [*d*,Å(*I*)(*hkl*)] are: 4.647(27)(111, 0$\bar{1}$1), 3.138(76)(002), 3.103(100)(120, 121), 3.027(20)(021), 2.960(81)(200), 2.158(19)(031, 302), 1.791(16)(320), 1.682(16)(114) and 1.584(17)(1$\bar{3}$3, 403). Bakakinite is a natural analogue of synthetic $Ca_2V_2O_7$. The mineral is named in honour of the outstanding Russian crystallographer and crystal chemist Vladimir Vasilievich Bakakin (born 1933).

Keywords: bakakinite; new mineral; calcium divanadate; fumarole sublimate; Tolbachik volcano

(Received 7 April 2023; accepted 26 May 2023; Accepted Manuscript published online: 7 June 2023; Associate Editor: Anthony R. Kampf)

Introduction

Divanadate minerals are not numerous in Nature. They are mainly represented by pyrovanadates, the oxysalts with anionic $[V_2O_7]^{4-}$ groups isolated from each other and composed of two V^{5+}-centred tetrahedra which share a bridging O atom. Among a dozen such minerals only volborthite, known since the 1830s, is relatively widespread. Typically, pyrovanadates (and natural divanadates in general) are hydrous minerals formed in supergene environments or in late, low-temperature hydrothermal assemblages. Except for volborthite $Cu^{3}V_2O_7(OH)_2{\cdot}2H_2O$ (Kashaev and Bakakin, 1968; Vladimirova *et al.*, 2021 and references therein) and the related minerals martyite $Zn_3V_2O_7(OH)_2{\cdot}2H_2O$ (Kampf and Steele, 2008) and karpenkoite $Co_3V_2O_7(OH)_2{\cdot}2H_2O$ (Kasatkin *et al.*, 2015), there are fianelite $Mn_2(V,As)_2O_7{\cdot}2H_2O$ (Brugger and Berlepsch, 1996), engelhauptite $KCu_3(V_2O_7)(OH)_2Cl$ (Pekov *et al.*, 2015), mesaite $CaMn_5^{2+}(V_2O_7)_3{\cdot}12H_2O$ (Kampf *et al.*, 2017) and donowensite $CaFe_2^{3+}(V_2O_7)_2{\cdot}3H_2O$ (Kampf *et al.*, 2022). For pintadoite the formula $Ca_2V_2O_7{\cdot}9H_2O$ is suggested, however, this mineral is poorly studied and has the IMA status Q – questionable (Pasero, 2023). The H-free natural pyrovanadates are represented by chervetite $Pb_2V_2O_7$ (Bariand *et al.*, 1963; Shannon and Calvo, 1973) and two modifications of $Cu_2V_2O_7$ – blossite and ziesite (Hughes and Birnie, 1980; Robinson *et al.*, 1987; Hughes and Brown, 1989; Krivovichev *et al.*, 2005); kainotropite $Cu_4Fe^{3+}O_2(V_2O_7)(VO_4)$ is the only known mineral containing both pyrovanadate $(V_2O_7)^{4-}$ and orthovanadate $(VO_4)^{3-}$ anions (Pekov *et al.*, 2020). Blossite, ziesite and kainotropite are endemics of volcanic fumaroles, as well as the new anhydrous calcium vanadate bakakinite (Cyrillic: бакакинит) described in the present paper. Bakakinite has the ideal, end-member formula $Ca_2V_2O_7$ and is a divanadate in terms of chemistry, however, from the crystal chemical viewpoint, it is not a pyrovanadate. This mineral contains more complex vanadate anionic groups – isolated tetramers $[V_4O_{14}]^{8-}$ built from 4-fold (tetrahedra) and 5-fold V^{5+}-centred polyhedra.

The new mineral is named in honour of the outstanding Russian crystallographer and crystal chemist Professor Vladimir Vasilievich Bakakin (born 1933) who works in Nikolaev Institute of Inorganic Chemistry of the Siberian Branch of the Russian Academy of Sciences, Novosibirsk. Prof. Bakakin made a significant contribution to the field of structural mineralogy. In particular, Kashaev and Bakakin (1968) first determined the crystal structure of volborthite and

Corresponding author: Igor V. Pekov; Email: igorpekov@mail.ru
Cite this article: Pekov I.V., Agakhanov A.A., Koshlyakova N.N., Zubkova N.V., Yapaskurt V.O., Britvin S.N., Vigasina M.F., Turchkova A.G. and Nazarova M.A. (2023) Bakakinite, $Ca_2V_2O_7$, a new mineral from fumarolic exhalations of the Tolbachik volcano, Kamchatka, Russia. *Mineralogical Magazine* **87**, 695–701. https://doi.org/10.1180/mgm.2023.42

showed that this mineral is a pyrovanadate and not an orthovanadate as it was assumed before.

Both the new mineral and its name (symbol Bkkn) have been approved by the Commission on New Minerals, Nomenclature and Classification of the International Mineralogical Association (IMA2022-046, Pekov *et al.*, 2022a). The holotype specimen is deposited in the systematic collection of the Fersman Mineralogical Museum of the Russian Academy of Sciences, Moscow with the catalogue number 98012.

Occurrence and general appearance

The specimens with the new mineral were collected by us in July 2021 from the Arsenatnaya fumarole, Second scoria cone of the Northern Breakthrough of the Great Tolbachik Fissure Eruption, Tolbachik volcano, Kamchatka peninsula, Far-Eastern Region, Russia, 55°41′N, 160°14′E, 1200 m elevation. This active fumarole that contains very rich and diverse high-temperature sublimate mineralisation has been described by Pekov *et al.* (2018) and Shchipalkina *et al.* (2020).

Bakakinite was found in several open pockets at the deepest (depths of 3–4 m under the day surface) and hottest zone of Arsenatnaya. The temperatures measured using a chromel–alumel thermocouple in these pockets during sampling varied from 430 to 490°C. We believe that bakakinite crystallised at temperatures not lower than 500°C. It can be deposited directly from hot gas as a volcanic sublimate, however, in our opinion, it seems more probably that the mineral was formed as a result of the interaction between fumarolic gas and basalt scoria. The latter could be a source of calcium which has very low volatility in such post-volcanic systems (Symonds and Reed, 1993).

Bakakinite occurs, sporadically in significant amounts, as a constituent of polymineralic exhalation incrustations together with anhydrite, svabite, pliniusite, schäferite, berzeliite, diopside, hematite and powellite. Minor amounts of baryte, fluorapatite, calciojohillerite, ludwigite, magnesioferrite, anorthite, titanite and esseneite also occur in this mineral assemblage. Cavernous polymineralic aggregates containing up to 25 vol.% bakakinite form thin (usually not thicker than 0.02 mm) crusts up to several cm^2 in area on anhydrite crystal crusts that cover basalt scoria altered by fumarolic gas to aggregates mainly consisting of diopside and hematite.

Bakakinite forms flattened crystals typically not larger than 10 μm, rarely up to 30 μm across and up to 5 μm thick. Some crystals are well-formed and complicated in shape (Fig. 1a), however, commonly bakakinite crystals are crude and distorted. The crystals, even with a well-developed outer shape, have skeletal (Fig. 1b) and/or blocky characters. Epitactic bakakinite overgrowths on svabite were observed (Fig. 1b). Clusters of bakakinite crystals are up to 0.1 mm across; in such clusters, bakakinite is intimately intergrown with other minerals, usually with anhydrite and svabite–pliniusite series members.

Physical properties and optical data

Bakakinite is transparent, colourless or pale yellow, with a white streak and strong vitreous lustre. It is brittle, cleavage or parting was not observed. The fracture is uneven (observed under the scanning electron microscope). The density value calculated using the averaged empirical formula is 3.463 g cm^{-3}.

The new mineral is transparent and optically anisotropic, however, its optical studies were carried out in reflected light due to high refractive indices. The mean refractive index calculated on the basis of the Gladstone–Dale equation is 1.93.

Under the microscope in reflected light, bakakinite is grey; pleochroism was not observed. Bireflectance is weak, $\Delta R = 1.2\%$ (589 nm). Anisotropy is very weak; internal reflections were not observed. The reflectance values measured in air using the SiC standard (Zeiss, No. 545) are given in Table 1.

Chemical composition

The composition of bakakinite was studied by electron microprobe using a Jeol JSM-6480LV scanning electron microscope equipped with an INCA-Wave 500 wavelength-dispersive spectrometer (Laboratory of Analytical Techniques of High Spatial Resolution, Dept. of Petrology, Moscow State University), with an acceleration voltage of 20 kV, a beam current of 20 nA and

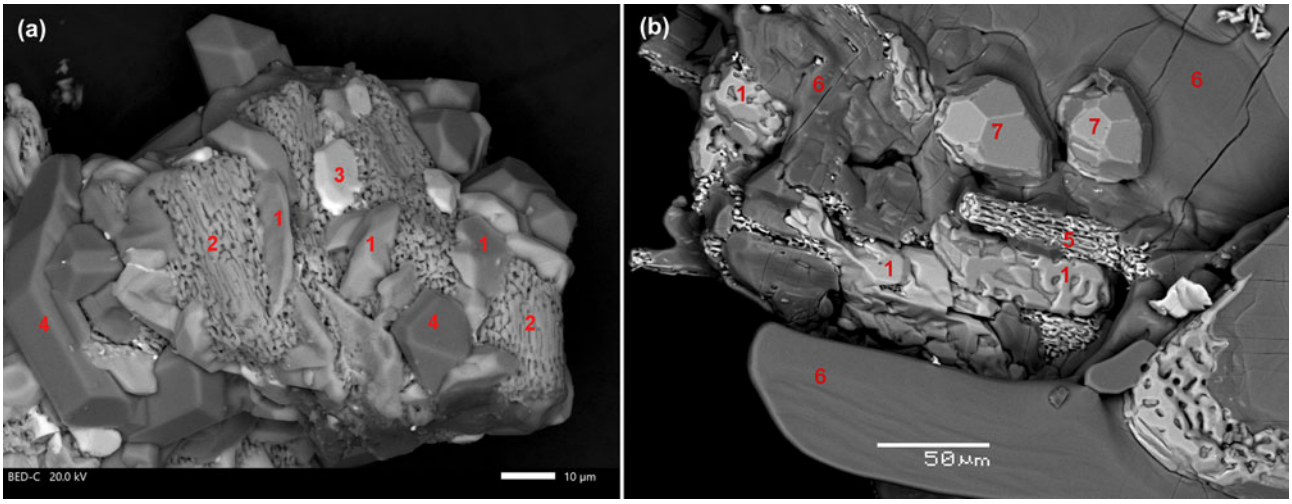

Figure 1. Morphology of crystals and aggregates of bakakinite and its relations with associated minerals: (a) flattened crystals of bakakinite (1) on pliniusite (2) with crystals of powellite (3) and diopside (4); (b) epitactic overgrowths of bakakinite skeletal crystals (1) on svabite (5) in association with anhydrite crusts (6) and schäferite crystals (7). Scanning electron microscopy image – back-scattered electron mode.

https://doi.org/10.1180/mgm.2023.42 Published online by Cambridge University Press

Table 1. The reflectance data of bakakinite.

λ (nm)	R_{max} (%)	R_{min} (%)	λ (nm)	R_{max} (%)	R_{min} (%)
400	18.2	16.6	560	14.8	13.0
420	17.8	15.6	580	14.8	13.6
440	14.9	13.6	**589**	**14.8**	**13.6**
460	13.9	12.6	600	14.9	13.6
470	**15.3**	**14.4**	620	14.9	13.7
480	15.3	13.9	640	14.9	13.9
500	14.7	13.5	**650**	**14.9**	**13.9**
520	14.3	13.2	660	15.5	14.1
540	14.3	12.8	680	15.8	14.4
546	**14.3**	**12.8**	700	14.1	13.5

The values for wavelengths (λ) recommended by the IMA Commission on Ore Mineralogy are marked in boldtype.

a 3 μm beam diameter. The standards used are listed in Table 2. Contents of other elements with atomic numbers >6 were below detection limits.

The chemical composition of bakakinite in wt.% is given in Table 2. The empirical formula calculated on the basis of 7 O atoms per formula unit is $(Ca_{1.99}Sr_{0.01})_{\Sigma 2.00}(V_{1.64}As_{0.28}P_{0.06}Si_{0.01}S_{0.01})_{\Sigma 2.00}O_7$. The simplified formula is $Ca_2(V,As)_2O_7$. The ideal, end-member formula of bakakinite is $Ca_2V_2O_7$ which requires CaO 38.14, V_2O_5 61.86, total 100 wt.%.

X-ray crystallography

Attempts to obtain single-crystal X-ray diffraction (XRD) data for bakakinite were unsuccessful due to the small size and low quality (skeletal and/or blocky character) of crystals.

Powder XRD data (Table 3) were collected with a Rigaku R-AXIS Rapid II single-crystal diffractometer equipped with cylindrical image plate detector (radius 127.4 mm) using Debye-Scherrer geometry, Co*K*α radiation (rotating anode with VariMAX microfocus optics), 40 kV, 15 mA and exposure of 15 min. Angular resolution of the detector is 0.045 2θ (pixel size 0.1 mm). The data were integrated using the software package *Osc2Tab* (Britvin *et al.*, 2017).

Despite the absence of single-crystal XRD data, it is clear that bakakinite is a natural analogue of a well-known synthetic calcium divanadate, $Ca_2V_2O_7$, of which the crystal structure was reported by Trunov *et al.* (1983) and Tong *et al.* (2011). Intimate intergrowths of bakakinite with other minerals hampered the Rietveld refinement of the crystal structure, however, its structural identity with synthetic $Ca_2V_2O_7$ found from powder XRD data is clear: see Discussion and Tables 3 and 4. Bakakinite is triclinic, with space group $P\bar{1}$. The unit-cell parameters are reported in Table 4.

Table 2. Chemical composition of bakakinite (in wt.%).

Constituent	Average (n = 9)	Range	S.D.	Probe standard
CaO	37.04	35.60–38.14	0.82	diopside
SrO	0.26	0.17–0.34	0.06	$SrSO_4$
SiO_2	0.16	0.11–0.23	0.05	diopside
P_2O_5	1.48	0.30–2.27	0.66	$KTiOPO_4$
V_2O_5	49.47	45.39–52.35	2.35	V
As_2O_5	10.85	8.38–14.57	2.08	GaAs
SO_3	0.35	0.17–0.75	0.22	FeS_2
Total	99.61			

S.D. = standard deviation

Table 3. Powder X-ray diffraction data (d in Å) of bakakinite and synthetic $Ca_2V_2O_7$.

Bakakinite*			Synthetic $Ca_2V_2O_7$		
I_{obs} (%)	d_{obs}	d_{calc}	I_{calc} (%)	d_{calc}	$h\ k\ l$
27	**4.647**	4.658, 4.616	8, 16	4.665, 4.608	111, 0$\bar{1}$1
5	4.273	4.287	4	4.310	$\bar{1}$10
10	3.299	3.296	8	3.310	201
12	3.264	3.259	10	3.261	$\bar{1}\bar{1}$1
76	**3.138**	3.144	65	3.149	002
100	**3.103**	3.108, 3.096	100, 97	3.105, 3.099	120, 121
20	**3.027**	3.029	17	3.039	021
81	**2.960**	2.964	75	2.979	200
3	2.536	2.535	5	2.540	122
10	2.417	2.421	8	2.434	$\bar{1}$21
12	2.375	2.379, 2.366	2, 11	2.386, 2.364	$\bar{1}$02, 1$\bar{2}$2
12	2.284	2.292, 2.270	5, 8	2.293, 2.272	030, $\bar{1}\bar{1}$2
19	**2.158**	2.160, 2.152	9, 12	2.165, 2.160	031, 302
5	2.086	2.096, 2.074	2, 4	2.099, 2.076	003, 2$\bar{1}$3
9	1.926	1.925	11	1.928	322
14	1.802	1.800	13	1.806	3$\bar{1}$3
16	**1.791**	1.790	11	1.793	320
10	1.765	1.763	12	1.767	2$\bar{1}$2
16	**1.682**	1.682	10	1.686	114
9	1.661	1.660	6	1.661	2$\bar{1}$4
5	1.627	1.626	3	1.628	304
6	1.617	1.616	7	1.619	314
8	1.602	1.602	3	1.602	1$\bar{4}$1
17	**1.584**	1.592, 1.580	8, 6	1.590, 1.586	1$\bar{3}$3, 403
7	1.555	1.554	4	1.553	240
6	1.548	1.548	2	1.550	242
7	1.514	1.513, 1.511	2, 2	1.511, 1.511	1$\bar{2}$4, 2$\bar{2}$4
3	1.460	1.457	5	1.461	2$\bar{4}$1
10	1.431	1.429	9	1.429	341
4	1.352	1.352	2	1.354	343
6	1.341	1.341	4	1.343	3$\bar{2}$2
	This work		JCPDS-ICDD, #72-2312 (calculated based on structure data by Trunov *et al.* (1983)		

*The powder X-ray diffraction pattern also contains lines with d = 3.492 [a], 2.904 [s], 2.842 [a,s], 2.822 [s] and 1.875 [a,s] Å which are overlapped reflections of bakakinite and anhydrite [a], svabite [s] or both these minerals [a,s]. The strongest reflections are marked in boldtype.

Raman spectroscopy

The Raman spectrum of bakakinite (Fig. 2) was obtained on a randomly oriented crystal using an EnSpectr R532 instrument with a green laser (532 nm) at room temperature. The output power of the laser beam was ~6 mW. The spectrum was processed using the EnSpectr expert mode program in the range from 4000 to 100 cm^{-1} with the use of a holographic diffraction grating with 1800 lines mm^{-1} and spectral resolution was 6 cm^{-1}. The diameter of the focal spot on the sample was ~10 μm. The backscattered Raman signal was collected with a 60× objective; signal acquisition time for a single scan of the spectral range was 1000 ms and the signal was averaged over 30 scans.

The assignment of bands in the Raman spectrum of bakakinite can be performed based on the data reported by Griffith and Wickins (1966), Nakamoto (1986), Hardcastle and Wachs (1991), Russu (2008) and Chong *et al.* (2019) and taking into account the presence of a complex anionic group $[V_4O_{14}]^{4-}$ in

https://doi.org/10.1180/mgm.2023.42 Published online by Cambridge University Press

Table 4. Crystal data of bakakinite and synthetic $Ca_2V_2O_7$ and $Ca_2As_2O_7$.

	Bakakinite	Synthetic $Ca_2V_2O_7$	Synthetic $Ca_2As_2O_7$
Crystal system	Triclinic	Triclinic	Monoclinic
Space group	$P\bar{1}$	$P\bar{1}$	$C2/m$
a (Å)	6.64(2)	6.667–6.670	7.049(3)
b (Å)	6.92(2)	6.920–6.921	9.297(7)
c (Å)	7.01(2)	7.016–7.018	4.885(9)
α (°)	86.59(7)	86.38–86.39	
β (°)	63.77(7)	63.84	101.27(6)
γ (°)	83.47(6)	83.64–83.67	
V (Å^3)	287.0(5)	288.8	314.0
Z	2	2	2
Source	This work	Trunov *et al.* (1983); Tong *et al.* (2011)	Pertlik (1980)

$Ca_2V_2O_7$ (Trunov *et al.*, 1983; Tong *et al.*, 2011), a synthetic end-member analogue of the mineral.

The Raman spectrum of synthetic $Ca_2V_2O_7$ (= $Ca_4[V_4O_{14}]$: for the structure data see below) reported by Russu (2008) is similar to the spectrum of bakakinite in its general pattern. However, unlike this synthetic vanadate, bakakinite contains admixed arsenic which partially substitutes vanadium. We cannot clearly identify the bands corresponding to As^{5+}–O vibrations due to overlap with bands of V^{5+}–O vibrations (Nakamoto, 1986), however, it is necessary to take into account the effect of the As admixture on the Raman spectrum. This probably results in the broadening of some bands in comparison with the spectrum of synthetic $Ca_2V_2O_7$ (Russu, 2008), but also other features. The position of an intense sharp band corresponding to ^{IV}M–O–^{V}M (superscript Roman numerals mean coordination numbers) stretching vibrations, which is at 944 cm^{-1} in a pure vanadate synthetic compound ($M = V^{5+}$) and at 928 cm^{-1} in bakakinite ($M = V^{5+} > As^{5+}$). A band at 928 cm^{-1} is related to ν($^{V}V^{5+}$–O–$^{IV}As^{5+}$) and ν($^{V}V^{5+}$–O–$^{IV}V^{5+}$), wide bands with maxima at 872, 845 cm^{-1} and at 789 and 775 cm^{-1} are assigned to symmetric (ν_1) and asymmetric (ν_3) vibrations, respectively, in $(VO_4)^{3-}$, $[V_2O_8]^{6-}$ and $(AsO_4)^{3-}$ groups. A strong band at 695 cm^{-1} and a weak band at 527 cm^{-1} correspond to vibrations of the (V–O–V) and (V–O–As), and the low-frequency shoulder of a band at 695 cm^{-1} may be connected with vibrations in $[V_2O_8]^{6-}$. The group of bands in the region of 480–300 cm^{-1} corresponds to overlapping split bending modes δ_2 and δ_4 of $(VO_4)^{3-}$ and $(AsO_4)^{3-}$ tetrahedra and bending modes in $[V_2O_8]^{6-}$ groups. The bands with frequencies below 300 cm^{-1} are assigned to translational modes of calcium cations (Ca–O) and lattice modes.

The Raman spectrum of bakakinite was obtained from a small (20 μm) flattened grain which overgrows pliniusite $Ca_5(VO_4)_3F$. The strongest band in the Raman spectra of pliniusite occurs at 868–873 cm^{-1} and the next in intensity band is situated at 350–356 cm^{-1} (Pekov *et al.*, 2022b). In the above-described bakakinite spectrum, we observe a strong broad band at 872 cm^{-1} and a weak low-frequency shoulder of a broad band with maximum at 386 cm^{-1}. We cannot exclude that the broadening of these bands may be a result of, in addition to the effect of admixed As^{5+}, the overlap of spectral bands of bakakinite (prevailing) and pliniusite (admixed).

Discussion

The ideal formula of bakakinite is $Ca_2V_2O_7$. However, all electron-microprobe analyses demonstrate some arsenic admixture. Synthetic $Ca_2V_2O_7$ (Trunov *et al.*, 1983; Tong *et al.*, 2011) and $Ca_2As_2O_7$ (Pertlik, 1980) are not isotypic. They significantly differ from one another in symmetry, unit-cell metrics (Table 4) and crystal structure (Fig. 3). In both structures the layers of Ca cations are connected *via* anionic units built by V^{5+}- or As^{5+}-centred polyhedra. Noteworthy, in the papers on synthetic $Ca_2V_2O_7$, the descriptions of Ca-centred polyhedra are slightly different: Trunov *et al.* (1983) characterised them as nine- and eight-fold polyhedra whereas Tong *et al.* (2011) described both crystallographically non-equivalent Ca polyhedra as nine-fold ones. The analysis of interatomic Ca–O distances shows that strongly elongated Ca–O distances (more than 2.9 Å) were included in the coordination spheres of Ca in both papers. For clarity and better comparison with $Ca_2As_2O_7$, we omit strongly

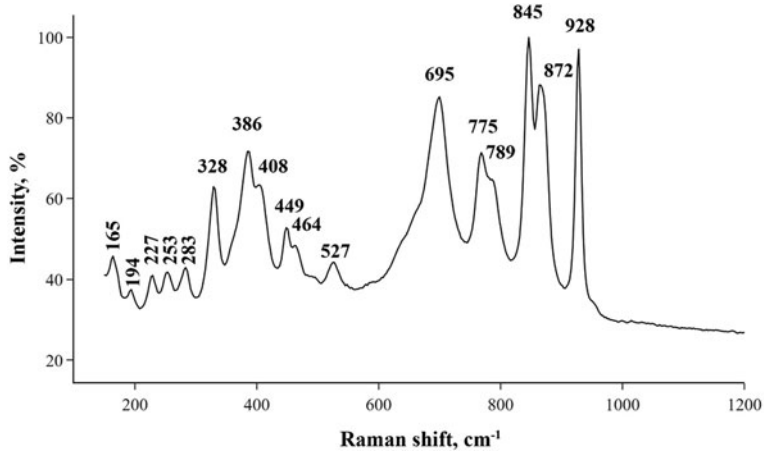

Figure 2. The Raman spectrum of bakakinite.

https://doi.org/10.1180/mgm.2023.42 Published online by Cambridge University Press

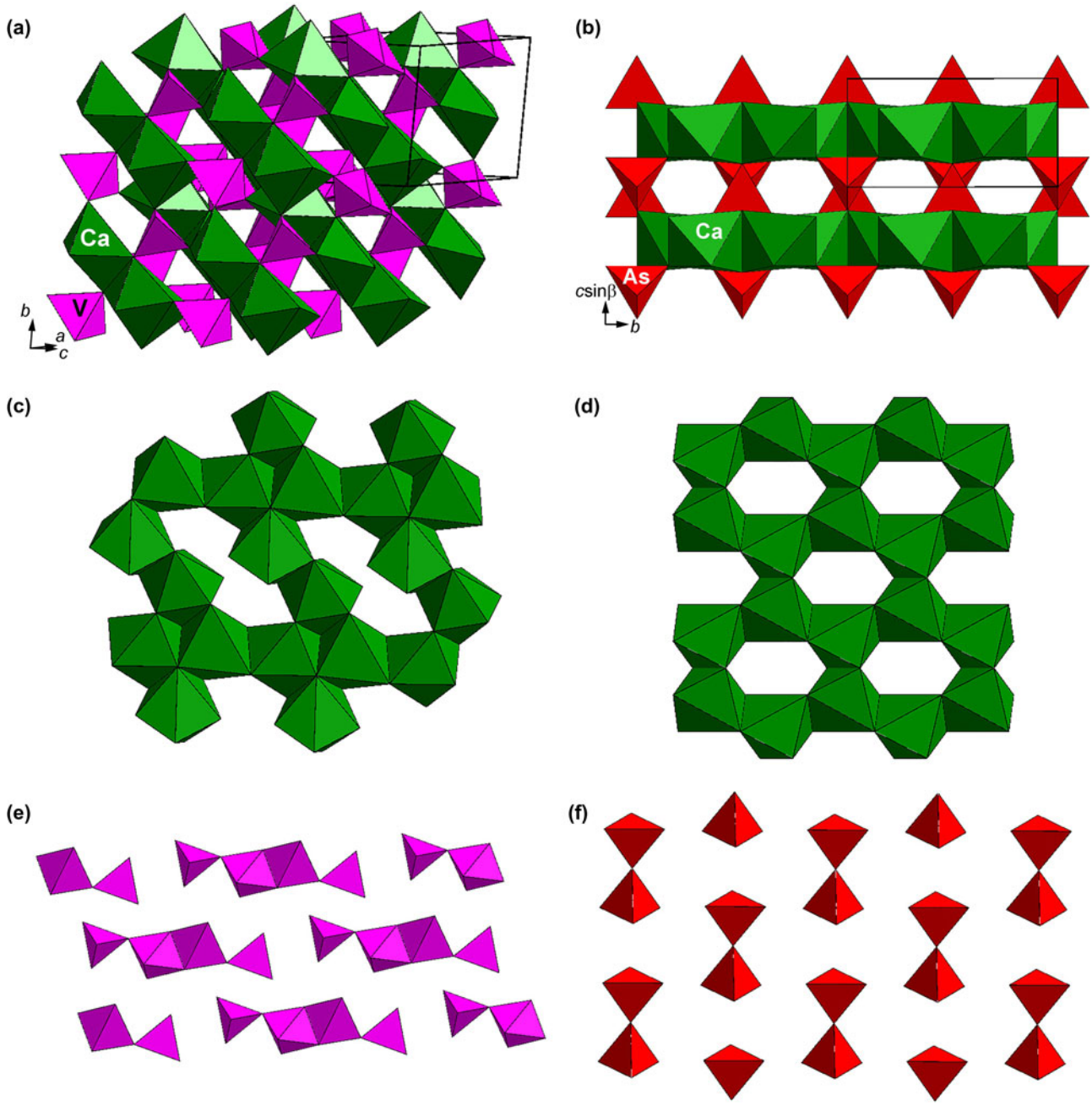

Figure 3. The crystal structures of synthetic analogue of bakakinite, $Ca_2V_2O_7$ (left column: drawn after Trunov *et al.* (1983); the unit cell is outlined) and $Ca_2As_2O_7$ (right column: drawn after Pertlik (1980); the unit cell is outlined): general view (a, b), the layers of Ca-centred polyhedra (c, d) and the arrangement of anionic $[V_4O_{14}]^{8-}$ tetramer units (e) and $[As_2O_7]^{4-}$ pyrogroups (f).

elongated Ca–O distances in the description below and in drawings given in Fig. 3. Following this approach, Ca cations in $Ca_2V_2O_7$ have distorted octahedral and seven-fold oxygen coordination whereas in $Ca_2As_2O_7$ calcium cations are located only in distorted octahedra. In both structures edge-sharing Ca-centred polyhedra form layers, but these layers in $Ca_2V_2O_7$ and $Ca_2As_2O_7$ strongly differ topologically (Figs 3c,d). The anionic units in these compounds are also quite different in arrangement and coordination of V and As atoms. In $Ca_2As_2O_7$, As^{5+} has only tetrahedral coordination whereas V^{5+} cations in $Ca_2V_2O_7$ centre tetrahedra and five-fold polyhedra (distorted trigonal bipyramids). In the structure of $Ca_2V_2O_7$ we see a linear anionic cluster, tetramer $[V_4O_{14}]^{8-}$, which is built of two edge-connected distorted trigonal bipyramids VO_5 (core of the cluster) and two VO_4 tetrahedra connected with these trigonal bipyramids *via* common vertices ('wings' of the cluster) (Fig. 3e). For this reason, Tong *et al.* (2011) wrote the formula of this vanadate as $Ca_4V_4O_{14}$ rather $Ca_2V_2O_7$. In the structure of $Ca_2As_2O_7$, arsenate tetrahedra form pyrogroups $[As_2O_7]^{4-}$, isolated from each other (Fig. 3f), i.e. it is a pyroarsenate.

The presence of pentacoordinated V^{5+} in $Ca_2V_2O_7$ prevents its isotypism with the formula analogues, numerous natural and synthetic compounds $Me_2T_2O_7$ (T = P, As and Si) in which T has only tetrahedral coordination. At the same time, our

https://doi.org/10.1180/mgm.2023.42 Published online by Cambridge University Press

electron-microprobe analyses show that bakakinite contains a distinct As admixture (Table 2) and, thus, we suggest that $Ca_2V_2O_7$ and $Ca_2As_2O_7$ can form a solid-solution series, at least, in the V-dominant region. The structure determinations were performed only for synthetic end-members (Pertlik, 1980; Trunov *et al.*, 1983; Tong *et al.*, 2011) and, thus, we do not know which chemical composition in this hypothetic series corresponds to the point of transition from the $Ca_2V_2O_7$ structure type (Fig. 3a) to the $Ca_2As_2O_7$ type (Fig. 3b). Unfortunately, we also know nothing on the distribution of V and admixed As between structure positions in bakakinite. If vanadium and arsenic occupy the sites with different coordination, then the increase of As^{5+} content could result in the formation of the hypothetical V–As-ordered bakakinite-type compound with the ideal formula Ca_2VAsO_7.

In the powder XRD data, bakakinite and synthetic $Ca_2V_2O_7$, being very close to one another (Table 3), differ strongly from $Ca_2As_2O_7$. In particular, the characteristic, low-angle region (d > 2.5 Å) of the powder XRD pattern of $Ca_2As_2O_7$ contains strong lines with d = 3.37, 3.34 and 2.77 Å and intensities I = 53, 100 (the strongest reflection of $Ca_2As_2O_7$) and 35%, respectively (Pertlik, 1980), which are absent in the powder XRD diagrams of bakakinite and synthetic $Ca_2V_2O_7$ (Table 3).

Of note, the crystal structure, unit-cell metrics and powder XRD pattern of another natural divanadate with large cations, chervetite $Pb_2V_2O_7$ (Shannon and Calvo, 1973) are quite different from those of both $Ca_2V_2O_7$ and $Ca_2As_2O_7$. All known polymorphs of $Cu_2V_2O_7$ including the minerals blossite and ziesite (Krivovichev *et al.*, 2005), also possess quite different structures.

Acknowledgements. We thank Evgeny Galuskin and two anonymous referees for their valuable comments. The mineralogical and spectroscopic studies of bakakinite and crystal chemical analysis by IVP, NVZ and MFV were supported by the Russian Science Foundation, grant no. 19-17-00050. The technical support by the SPbSU X-Ray Diffraction Resource Center in the powder XRD study is acknowledged.

Competing interests. The authors declare none.

References

Bariand P., Chantret F., Pouget R. and Rimsky A. (1963) Une nouvelle éspèce minérale: la chervetite, pyrovanadate de plomb $Pb_2V_2O_7$. *Bulletin de la Société Française de Minéralogie et de Cristallographie*, **86**, 117–120 [in French].

Britvin S.N., Dolivo-Dobrovolsky D.V. and Krzhizhanovskaya M.G. (2017) Software for processing the X-ray powder diffraction data obtained from the curved image plate detector of Rigaku RAXIS Rapid II diffractometer. *Zapiski Rossiiskogo Mineralogicheskogo Obshchestva*, **146**, 104–107 [in Russian].

Brugger J. and Berlepsch P. (1996) Description and crystal structure of fianelite, $Mn_2V(V,As)O_7{\cdot}2H_2O$, a new mineral from Fianel, Val Ferrera, Graubünden, Switzerland. *American Mineralogist*, **81**, 1270–1276.

Chong S., Aksenov S.M., Dal Bo F., Perry S.N., Dimakopoulou F. and Burns P.C. (2019) Framework polymorphism and modular crystal structures of uranyl vanadates of divalent cations: synthesis and characterization of $M(UO_2)(V_2O_7)$ (M = Ca, Sr) and $Sr_3(UO_2)(V_2O_7)_2$. *Zeitschrift für Anorganische und Allgemeine Chemie*, **645**, 981–987.

Griffith W.P. and Wickins T.D. (1966) Raman studies on species in aqueous solutions. Part I. The vanadates. *Journal of the Chemical Society A: Inorganic, Physical, Theoretical*, **1966**, 1087–1090.

Hardcastle F.D. and Wachs I.E. (1991) Determination of vanadium-oxygen bond distances and orders by Raman spectroscopy. *The Journal of Physical Chemistry*, **95**, 5031–5041.

Hughes J.M. and Birnie R.W. (1980) Ziesite, β-$Cu_2V_2O_7$, a new copper vanadate and fumarole temperature indicator. *American Mineralogist*, **65**, 1146–1149.

Hughes J.M. and Brown M.A. (1989) The crystal structure of ziesite, β-$Cu_2V_2O_7$, a thortveitite-type structure with a non-linear X-O-X inter-tetrahedral bond. *Neues Jahrbuch für Mineralogie, Monatshefte*, **1989**, 41–47.

Kampf A.R. and Steele I.M. (2008) Martyite, a new mineral species related to volborthite: description and crystal structure. *The Canadian Mineralogist*, **46**, 687–692.

Kampf A.R., Nash B.P., Marty J., Hughes J.M. (2017) Mesaite, $CaMn_5^{2+}(V_2O_7)_3{\cdot}12H_2O$, a new vanadate mineral from the Packrat mine, near Gateway, Mesa County, Colorado, USA. *Mineralogical Magazine*, **81**, 319–327.

Kampf A.R., Hughes J.M., Nash B.P. and Smith J.B. (2022) Donowensite, $Ca(H_2O)_3Fe_2^{3+}(V_2O_7)_2$, and mikehowardite, $Fe_4^{3+}(V^{5+}O_4)_4(H_2O)_2{\cdot}H_2O$, two new vanadium minerals from the Wilson Springs Vanadium Mine, Wilson Springs, Arkansas, U.S.A. *The Canadian Mineralogist*, **60**, 543–554.

Kasatkin A.V., Plášil J., Pekov I.V., Belakovskiy D.I., Nestola F., Čejka J., Vigasina M.F., Zorzi F. and Thorne B. (2015) Karpenkoite, $Co_3(V_2O_7)(OH)_2{\cdot}2H_2O$, a cobalt analogue of martyite from the Little Eva mine, Grand County, Utah, USA. *Journal of Geosciences*, **60**, 251–257.

Kashaev A.A. and Bakakin V.V. (1968) Crystal structure of volborthite $Cu_3(OH)_2V_2O_7{\cdot}2H_2O$. *Doklady Akademii Nauk SSSR*, **181**, 967–969 [in Russian].

Krivovichev S.V., Filatov S.K., Cherepansky P.N., Armbuster T. and Pankratova O.Y. (2005) Crystal structure of γ-$Cu_2V_2O_7$ and its comparison to blossite (α-$Cu_2V_2O_7$) and ziesite (β-$Cu_2V_2O_7$). *The Canadian Mineralogist*, **43**, 671–677.

Nakamoto K. (1986) *Infrared and Raman Spectra of Inorganic and Coordination Compounds*. John Wiley & Sons, New York.

Pasero M. (2023) *The New IMA List of Minerals*. International Mineralogical Association Commission on New Minerals, Nomenclature and Classification (IMA–CNMNC). http://cnmnc.main.jp/.

Pekov I.V., Siidra O.I., Chukanov N.V., Yapaskurt V.O., Britvin S.N., Krivovichev S.V., Schüller W. and Ternes B. (2015) Engelhauptite, $KCu_3(V_2O_7)(OH)_2Cl$, a new mineral species from Eifel, Germany. *Mineralogy and Petrology*, **109**, 705–711.

Pekov I.V., Koshlyakova N.N., Zubkova N.V., Lykova I.S., Britvin S.N., Yapaskurt V.O., Agakhanov A.A., Shchipalkina N.V., Turchkova A.G. and Sidorov E.G. (2018) Fumarolic arsenates – a special type of arsenic mineralization. *European Journal of Mineralogy*, **30**, 305–322.

Pekov I.V., Zubkova N.V., Yapaskurt V.O., Polekhovsky Yu.S., Britvin S.N., Turchkova A.G., Sidorov E.G. and Pushcharovsky D.Yu. (2020) Kainotropite, $Cu_4Fe^{3+}O_2(V_2O_7)(VO_4)$, a new mineral with a complex vanadate anion from fumarolic exhalations of the Tolbachik volcano, Kamchatka, Russia. *The Canadian Mineralogist*, **58**, 155–165.

Pekov, I.V., Agakhanov, A.A., Koshlyakova, N.N., Zubkova, N.V., Yapaskurt, V.O., Britvin, S.N., Vigasina, M.F., Turchkova, A.G. and Nazarova, M.A. (2022a) Bakakinite, IMA 2022-046. CNMNC Newsletter 69; *Mineralogical Magazine*, **86**, https://doi.org/10.1180/mgm.2022.115.

Pekov I.V., Koshlyakova N.N., Zubkova N.V., Krzątała A., Belakovskiy D.I., Galuskina I.O., Galuskin E.V., Britvin S.N., Sidorov E.G., Vapnik Y. and Pushcharovsky D.Yu. (2022b) Pliniusite, $Ca_5(VO_4)_3F$, a new apatite-group mineral and the novel natural ternary solid-solution system pliniusite–svabite–fluorapatite. *American Mineralogist*, **107**, 1626–1634.

Pertlik F. (1980) Die Kristallstruktur von $Ca_2As_2O_7$. *Monatshefte für Chemie*, **111**, 399–405.

Robinson P.D., Hughes J.M. and Malinconico M.L. (1987) Blossite, α-$Cu_2^{2+}V_2^{5+}O_7$, a new fumarolic sublimate from Izalco volcano, El Salvador. *American Mineralogist*, **72**, 397–400.

Russu S. (2008) *High-Throughput Synthesis and Characterization of Vanadium Mixed Metal Oxide Pigments Using Synchrotron Radiation*. PhD Thesis, University of Southampton, UK, 146 pp.

Shannon R.D. and Calvo C. (1973) Refinement of the crystal structure of synthetic chervetite, $Pb_2V_2O_7$. *Canadian Journal of Chemistry*, **51**, 70–76.

Shchipalkina N.V., Pekov I.V., Koshlyakova N.N., Britvin S.N., Zubkova N.V., Varlamov D.A. and Sidorov E.G. (2020) Unusual silicate mineralization in fumarolic sublimates of the Tolbachik volcano, Kamchatka, Russia – Part 1: Neso-, cyclo-, ino- and phyllosilicates. *European Journal of Mineralogy*, **32**, 101–119.

Symonds R.B. and Reed M.H. (1993) Calculation of multicomponent chemical equilibria in gas-solid-liquid systems: calculation methods, thermochemical data, and applications to studies of high-temperature volcanic gases with examples from Mount St. Helens. *American Journal of Science*, **293**, 758–864.

Tong Y.-P., Luo G.-T., Jin Z. and Lin Y.-W. (2011) Synthesis, structure and theoretical investigations of an alkaline earth vanadate oxide compound ($Ca_4V_4O_{14}$): electronic, optical and chemical bond properties. *Australian Journal of Chemistry*, **64**, 973–977.

Trunov V.K., Velikodnyi Yu.A., Murasheva E.V. and Zhuravlev, V.D. (1983) The crystal structure of calcium pyrovanadate. *Doklady Akademii Nauk SSSR*, **270**, 886–887 [in Russian].

Vladimirova V.A., Siidra O.I., Ugolkov V.L., Bubnova R.S. (2021) Refinement of the crystal structure and features of the thermal behavior of volborthite $Cu_3V_2O_7(OH)_2{\cdot}2H_2O$ from the Tyuya-Muyun Deposit, Kyrgyzstan. *Zapiski Rossiiskogo Mineralogicheskogo Obshchestva*, **150**, 115–133 [in Russian].

https://doi.org/10.1180/mgm.2023.42 Published online by Cambridge University Press